

---

# Noisy Spiking Actor Network for Exploration

---

Ding Chen<sup>1,2</sup> Peixi Peng<sup>3,2</sup> Tiejun Huang<sup>3</sup> Yonghong Tian<sup>3,2</sup>

## Abstract

As a general method for exploration in deep reinforcement learning (RL), NoisyNet can produce problem-specific exploration strategies. Spiking neural networks (SNNs), due to their binary firing mechanism, have strong robustness to noise, making it difficult to realize efficient exploration with local disturbances. To solve this exploration problem, we propose a noisy spiking actor network (NoisySAN) that introduces time-correlated noise during charging and transmission. Moreover, a noise reduction method is proposed to find a stable policy for the agent. Extensive experimental results demonstrate that our method outperforms the state-of-the-art performance on a wide range of continuous control tasks from OpenAI gym.

## 1. Introduction

In recent years, deep reinforcement learning (RL) has surpassed human-level control in a wide range of tasks (Schrittwieser et al., 2020). The agent trained by deep RL can perceive the environment and interact with it, autonomously making plans, decisions, and actions based on tasks, which is considered a technological route for embodied intelligence. However, the limited on-board energy resources on mobile devices such as robots are unable to meet the requirements of deep learning algorithms for computational resources. Compared to the human brain, existing computing systems require at least an order of magnitude more energy consumption to perform the same task (Cox & Dean, 2014). Inspired by the brain, neuromorphic computing using spike-driven communication is proposed to solve the high energy consumption problem faced by current deep learning algorithms. The rapid development of neuromorphic hardware leads numerous algorithm researchers to invest in the study of spiking neural networks (SNNs). Due to their distinctive properties, such as extremely low energy

consumption, spatiotemporal information processing capability, and high biological plausibility (Roy et al., 2019), there have been some recent works using SNNs for RL (i.e. spike-based RL), providing an energy-efficient solution for continuous control tasks.

For the exploration-exploitation trade-off of RL, many researchers have proposed efficient methods for exploration, among which most exploration heuristics rely on random perturbations of the agent’s policy, such as  $\epsilon$ -greedy, to induce novel behaviors (Sutton & Barto, 2018). However, such local disturbances are difficult for the agent to effectively explore in diverse environments. Therefore, Fortunato et al. (2018) proposed NoisyNet, which introduces parametric noise in network weights to generate problem-specific exploration strategies. However, due to its binary firing mechanism, SNN has strong robustness to noise, so local perturbations of input or network weights have a relatively small impact on the agent’s policy (Patel et al., 2019), posing greater challenges to exploration based on parametric noise in network weights.

To develop a general method for exploration of spike-based RL, the key issue is to incorporate noise into the spiking neural model. Spiking neurons with noise-perturbed dynamics are considered more biologically plausible, as ion channel fluctuations and synaptic transmission randomness can lead to noisy sub-threshold membrane voltage (Verveen & DeFelice, 1974; Stein et al., 2005). To further enhance the impact of noise on the policy, we propose a new noisy spiking neural model that introduces random noise in both charging and transmission. Due to the fact that noise only exists during training for exploration, the trained SNN still emits binary signals during evaluation, meeting the deployment requirements of neuromorphic hardware. To ensure that the agent finds a stable policy after sufficient exploration, we propose a noise reduction method for non-spiking neurons (Chen et al., 2024) on the output layer, inspired by (Han et al., 2022). In many tasks, we need to coordinate behavior over multiple steps to reach a sufficiently different state, but the exploration behavior of white noise cannot meet this requirement. Moreover, we hope that the noise can balance global consistency and local randomness in the internal temporal calculation of SNNs. Therefore, we introduce colored noise (Eberhard et al., 2022) to concatenate action sequence within an episode with spike-train within SNNs, enabling

---

<sup>1</sup>Department of Computer Science and Engineering, Shanghai Jiao Tong University, Shanghai, China <sup>2</sup>Network Intelligence Research, PengCheng Laboratory, Shenzhen, China <sup>3</sup>Department of Computer Science and Technology, Peking University, Beijing, China. Correspondence to: Yonghong Tian <yh-tian@pku.edu.cn>.

spike-based RL algorithms to work well both on environments where white noise is enough, and on those which require more exploration. The main contributions of this paper are summarized as follows:

1. A novel spiking actor network using noisy spiking neural models, called NoisySAN, is proposed. To our best knowledge, it is the first work for exploration of spike-based RL algorithms. The experimental results show that our method outperforms the state-of-the-art performance on extensive continuous control tasks from OpenAI gym.
2. A novel noise reduction method for non-spiking neurons on the output layer is proposed, which stabilizes the agent’s policy after thorough exploration and further improves performance.
3. A novel noise generation method for spike-based RL is proposed, which for the first time concatenates action sequence within an episode with spike-train within deep SNNs. The experimental results show that pink noise is superior to all other noise types, and the temporal concatenation helps improve performance.

## 2. Related Work

### 2.1. Spiking Actor Networks

Tang *et al.* (2020) first propose the spiking actor network, which, together with a deep critic network, utilizes the DDPG algorithm (Gu *et al.*, 2016) for collaborative training. Based on this work, PopSAN (Tang *et al.*, 2021) is proposed to improve the representation ability of SNNs through population coding. For the same purpose, Zhang *et al.* (2022) propose a multiscale dynamic coding improved spiking actor network (MDC-SAN). Through membrane voltage coding and intra-layer connections, ILC-SAN (Chen *et al.*, 2024) becomes the first fully spiking neural network to achieve the same level of performance as the mainstream deep RL algorithms. We use ILC-SAN as a benchmark and utilize the noisy spiking neural model to achieve effective exploration.

### 2.2. Exploration Methods in Reinforcement Learning

In RL, random variables are usually introduced into policies for exploration. The  $\epsilon$ -greedy algorithm is commonly used for RL tasks with discrete action space. For RL tasks with continuous action space, entropy regularization and action noise are two commonly used exploration methods. The former is used in stochastic policies (Haarnoja *et al.*, 2018), while the latter is used in deterministic policies (Fujimoto *et al.*, 2018) and injected into the action selection process, where action noise could be drawn from any random process, usually white noise (drawn from Gaussian

distributions) or Ornstein-Uhlenbeck (OU) noise. Recently, colored noise (Eberhard *et al.*, 2022) is proposed as a general family of temporally correlated noise processes, where a parameter  $\beta$  is used to control the correlation strength, such as  $\beta = 0$  for white noise and  $\beta = 2$  for red noise, which also known as Brownian motion and closely related to OU noise. They found that noises with intermediate temporal correlation (pink noise,  $\beta = 1$ ) outperform all other noise types when averaged across a selection of standard benchmarks. Moreover, Hollenstein *et al.* (2022) found that the noise configuration, noise type and noise scale, have an important impact on learning.

The action noise is independent of the state, so there may be differences in the output results obtained by inputting the same state. Therefore, parameter space noise (Plappert *et al.*, 2018) is proposed, which is added to the agent’s parameters at the beginning of each episode and remains fixed throughout one episode, achieving stable exploration. Unlike adaptive variance adjustment of parameter space noise, NoisyNet (Fortunato *et al.*, 2018) learns noise parameters along with network weights through gradient descent, which is used in an integrated method called Rainbow (Hessel *et al.*, 2018) and plays a role in improving overall performance. To make the agent learn stable policies, NROWAN-DQN (Han *et al.*, 2022) develop a novel noise reduction method for NoisyNet-DQN.

The above exploration methods, except for parameter space noise and NoisyNet, have little difference between ANNs and SNNs. Therefore, we focus on how to integrate noise into SNNs. Our method is closer to the actor network in NoisyNet-A3C, but our noise parameters are in the neural model rather than in the network weights. For efficient exploration, we set the noise parameters of spiking neurons to be fixed, rather than learnable in NoisyNet. Inspired by NROWAN-DQN, we add a loss term related to the noise parameters of non-spiking neurons in the output layer and adjust the weight of this loss term online based on the episode reward. Moreover, the noise of our method is drawn from colored noise, instead of Gaussian distributions in NoisyNet.

### 2.3. Noisy Spiking Neural Networks

Noisy SNNs are commonly used for image classification tasks, adding Gaussian white noise in the charging dynamics of spiking neural models. Jiang and Zhang (2023) train a single-step SNN by approximating the neural potential distribution with white noise, and then convert the single-step SNN to a multi-step SNN. The introduction of white noise leads to a significant improvement in accuracy after conversion. Zhang *et al.* (2023) inject white noise with learnable variance into the training process for better robustness. Ma *et al.* (2023) propose a noise-driven learning rule, which achieves competitive performance and improve robustness

against challenging disturbances. Unlike these works, we use time-correlated noise to drive exploration behavior in RL and add random noise in both subthreshold dynamics and spike transmission.

### 3. Method

In this paper, we focus on efficient exploration of spiking actor networks in diverse control tasks. In this section, we first introduce the spiking neural model and the non-spiking neural model, as well as their discrete dynamics. After that, we propose their noise versions. Then, we present the implemented details of NoisySAN. Next, we propose the noise generation method and the noise reduction method. Finally, we present the training details of NoisySAN.

#### 3.1. Neural Models

Spiking neurons is the basic computing unit of SNNs. According to the order of charging, firing, and resetting, the dynamics of spiking neurons can usually be described as:

$$H_t = f(V_{t-1}, X_t), \quad (1)$$

$$S_t = \Theta(H_t - V_{th}), \quad (2)$$

$$V_t = H_t(1 - S_t) + V_{reset}S_t, \quad (3)$$

where  $H_t$  and  $V_t$  represent the membrane voltage after charging and firing at time-step  $t$ , respectively.  $X_t$  means the external input, and  $S_t$  denotes the output spike at time-step  $t$ .  $V_{th}$  represents the threshold voltage and  $V_{reset}$  represents the membrane reset voltage. The function  $f(\cdot)$  describes various subthreshold dynamics of different neurons.  $\Theta(x)$  is the Heaviside step function, which is defined by  $\Theta(x) = 1$  for  $x \geq 0$  and  $\Theta(x) = 0$  for  $x < 0$ . Note that  $V_0 = V_{reset}$ ,  $S_0 = 0$ . The dynamics described by the Eq. (3) are called the hard reset.

Non-spiking neurons can be considered as a special case of spiking neurons, and their dynamics can be simplified as:

$$V_t = f(V_{t-1}, X_t). \quad (4)$$

By utilizing the membrane voltage coding of non-spiking neurons (Chen et al., 2024), we can convert the spike-train in SNNs into a continuous action.

For exploration, we introduce random noise and propose novel noisy versions of these models (Figure 1). The modification of noisy spiking neurons can be described as:

$$H_t = f(V_{t-1}, X_t) + \sigma_v \odot \varepsilon_v, \quad (5)$$

$$\tilde{S}_t = S_t + \sigma_s \odot \varepsilon_s, \quad (6)$$

where  $\sigma_v$  and  $\sigma_s$  denote the noise parameters.  $\varepsilon_v$  and  $\varepsilon_s$  mean the noise drawn from any random process.  $\tilde{S}_t$  represent noisy signal during spike transmission, which occurs

after firing and participates in the input current calculation of downstream neurons. Note that Eq. (5) is a rewrite of Eq. (1), and the firing and resetting dynamics of noisy spiking neurons remain unchanged, namely Eq. (2), (3). In addition, the dynamics of noisy non-spiking neurons can be described as:

$$V_t = f(V_{t-1}, X_t) + \sigma_v \odot \varepsilon_v. \quad (7)$$

#### 3.2. Noisy Spiking Actor Network

In this subsection, we present the implemented details of our NoisySAN. First, we use a population encoder with different learnable Gaussian receptive fields to encode each state dimension into several spike-trains. Secondly, these spike-trains propagate forward in the backbone SNN to obtain output spike-trains. For a task with  $N_A$ -dimensional actions, we equally divide the spiking neurons of the last layer into  $N_A$  output population with intra-layer connections. Finally, each output population has a corresponding population decoder, which projects the spike-trains into the corresponding action dimension using the last membrane voltage after every  $T$  simulation time-steps ( $V_T$ ). For more details about the network structure, please refer to (Chen et al., 2024).

In our NoisySAN, we use noisy current-based LIF (CLIF) neurons in the backbone SNN and noisy integrated neurons in the population decoder. Compared to the spiking neurons mentioned in Section 3.1, noisy CLIF neurons contain an additional current term  $C_t$ . Therefore, Eq. (5) needs to be rewritten as:

$$C_t = \alpha_C C_{t-1} + X_t, \quad (8)$$

$$H_t = \alpha_V V_{t-1} + C_t + \sigma_v \odot \varepsilon_v, \quad (9)$$

where  $\alpha_C$  and  $\alpha_V$  are the current and voltage decay factors. Note that  $C_0 = 0$ . According to Eq. (7), the dynamics of noisy integrated neurons can be described as:

$$V_t = V_{t-1} + X_t + \sigma_v \odot \varepsilon_v. \quad (10)$$

#### 3.3. Noise Generation Method

Colored noise is a stochastic process with parameter  $\beta$ , and the signal  $\varepsilon(t)$  drawn from it have the property that the power spectral density (PSD) satisfies  $|\hat{\varepsilon}(f)|^2 \propto f^{-\beta}$ , where  $\hat{\varepsilon}(f) = \mathcal{F}[\varepsilon(t)](f)$  means the Fourier transform of  $\varepsilon(t)$  and  $f$  denotes the frequency.

The parameter  $\beta$  controls the temporal correlation of the signal. If  $\beta = 0$ , the signal is uncorrelated. This noise is called white noise in analogy to light. Similarly, red noise ( $\beta = 2$ ) represent the signal has more weight on lower frequencies. The complete noise signal of an episode can be sampled at once, and then colored noise with specified variance can be generated according to Eq. (5), (6).

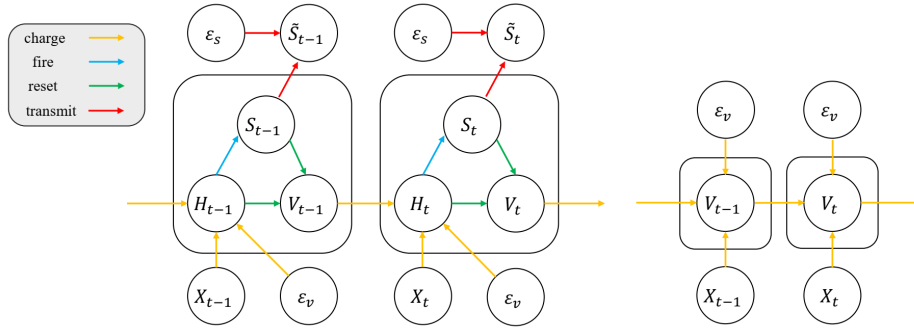


Figure 1. The general discrete noisy neural model (Left) Noisy spiking neural model. (Right) Noisy non-spiking neural model.

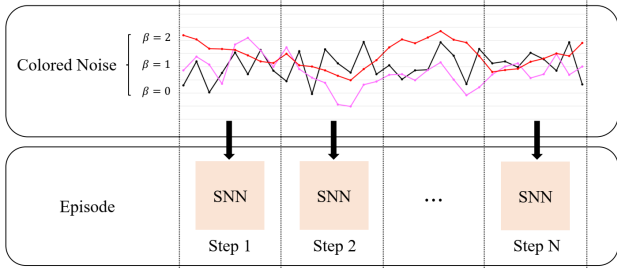


Figure 2. The noise generation method. The complete colored noise of an episode is first divided into  $N$  segments according to the maximum length of the episode, and then used in noisy neurons of the SNN at time-step  $t$ .

Due to the simulation time  $T$  of SNNs in each action selection, we use colored noise to concatenate action sequence within a episode with spike-train within SNNs for the consistency of the exploration strategy (Figure 2). For effective exploration, each noisy spiking neuron has two complete noise signals with a length of  $N \cdot T$  for  $\epsilon_v$  and  $\epsilon_s$ , where  $N$  denotes the maximum length of the episode. And each noisy non-spiking neuron has a complete noise signal with a length of  $N \cdot T$  for  $\epsilon_v$ .

### 3.4. Noise Reduction Method

Although NoisyNet suggests that the agent does not necessarily evolve towards a deterministic solution as one might have expected, experimental results have shown that in some cases, high noise parameters also limit the efficiency of algorithms (Han et al., 2022). Similar to action noise, the noise generated by non-spiking neurons directly affects actions. As (Hollenstein et al., 2022) recommends reducing the action noise scaling factor over the training time, we propose a noise reduction method for non-spiking neurons to achieve abundant exploration and efficient training.

To achieve this goal, we use the sum of the original loss function of SANs and the noise variance of the non-spiking neurons as the new loss function:

$$\mathcal{L}_{new} = \mathcal{L}_{old} + \frac{k}{N_A} \sum_{i=1}^{N_A} \sigma_i^2, \quad (11)$$

where  $N_A$  denotes the action dimension and  $k$  is the coefficient that controls the update ratio between the original gradient update direction and the noise reduction direction. When the episode reward is low, a small  $k$  can make the agent tend to explore for a better policy. When the episode reward is high, a big  $k$  can make the agent tend to exploit for a larger episode reward. Therefore, we dynamically adjust the value of  $k$  based on the reward and the task:

$$k = k_0 \cdot \frac{R_{eval} - R_{min}}{R_{max} - R_{min}}, \quad (12)$$

where  $R_{eval}$  denotes the evaluation results after every 10k training steps.  $R_{max}$  denotes the maximum reward and  $R_{min}$  denotes the minimum reward, respectively. Due to the difficulty in obtaining these two values, we set  $R_{min}$  to zero and  $R_{max}$  to a value slightly higher than the state-of-the-art performance.  $k_0$  is the factor that controls the magnitude of the loss term.

### 3.5. NoisySAN embedded into TD3

Our NoisySAN is functionally equivalent to a deep actor network (DAN), which can be trained in conjunction with a deep critic network using TD3 algorithms (Fujimoto et al., 2018). Before each episode starts, we sample the complete noise signal at once, which is used for exploration. During exploration, training samples are collected into the replay buffer. To update the noise parameters of NoisySAN, the random noise used for this action selection is also recorded in each transition. Noted that we use target policy smoothing regularization (Fujimoto et al., 2018) to update the deep critic network with noiseless NoisySAN.

Table 1. Max average rewards over 10 random seeds for DAN, NoisySAN and other SANs.

TASK	DAN	POP SAN	MDC-SAN	ILC-SAN	NOISYSAN
ANT-V3	5472±653	5264±920	5311±806	5339±503	5524±415
HALFCHEETAH-V3	10471±1695	9419±1600	10323±1669	10789±922	10723±817
HOPPER-V3	3520±105	230±52	1824±1738	3125±1096	3356±652
WALKER2D-V3	4999±842	4023±1497	4670±555	4712±419	4747±654
HUMANOID-V3	3681±2258	5664±271	4775±2302	5486±169	5578±291
HUMANOIDSTANDUP-V2	129271±13021	145057±6194	157959±21225	146480±8828	161811±17778
INVERTEDDOUBLEPENDULUM-V2	8425±2950	9324±2	9330±4	9327±2	9322±5
BIPEDALWALKER-V3	194±146	249±111	223±117	196±142	295±7
APR	100.00%	97.28%	102.31%	107.22%	<b>116.63%</b>

Table 2. Max average rewards over 10 random seeds for NoisySANs and ILC-SANs using pink noise or noisy layers.

TASK	NOISYSAN	ILC-SAN+PN	ILC-SAN+NL
ANT-V3	5524±415	5640±397	4940±751
HALFCHEETAH-V3	10723±817	10179±916	7629±2929
HOPPER-V3	3356±652	3222±1037	2888±1037
WALKER2D-V3	4747±654	4861±675	4035±655
HUMANOID-V3	5578±291	5724±278	5598±192
HUMANOIDSTANDUP-V2	161811±17778	163034±29159	163448±25405
INVERTEDDOUBLEPENDULUM-V2	9322±5	9326±3	6815±4051
BIPEDALWALKER-V3	295±7	236±125	185±136
APR	<b>116.63%</b>	112.88%	97.58%

### 4. Experiments

In this section, we first compare the performance of NoisySANs with other SANs on eight continuous control tasks from OpenAI gym. After that, we compare the performance of NoisySANs with ILC-SANs using pink noise (Eberhard et al., 2022) or noisy layers (Fortunato et al., 2018) on these tasks. Then we analyze the effects of different parameter  $\beta$  on performance, and evaluate the influence of each component in noisy spiking neurons. Finally, we demonstrate the effectiveness of the noise generation method and the noise reduction method through ablation study and comparison experiment. In addition, our experiments are built upon the open-source code of PopSAN.

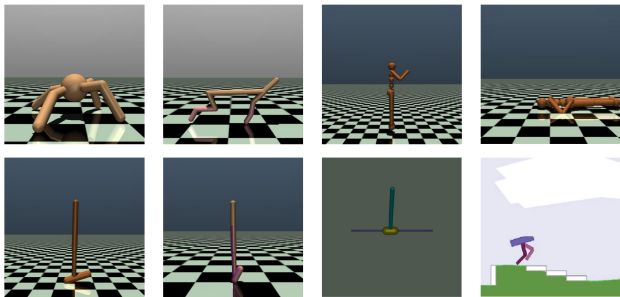


Figure 3. Eight continuous control tasks from OpenAI gym.

### 4.1. Experimental Settings

We evaluated our method on OpenAI gym tasks, which are commonly used as benchmarks for continuous control algorithms. All the tasks used are shown in Figure 3. To ensure reproducibility, each of models used is trained for 10 rounds, corresponding to 10 random seeds. In each round, the task is trained for 1 million steps and evaluated every 10k steps, where the average reward over 10 episodes using deterministic policies is reported, and used for the noise reduction method. Note that deterministic policies represent not using noise in NoisySAN. Each episode can last up to 1000 execution steps, i.e.  $N = 1000$  in the noise generation method. Moreover, the factor  $k_0$  is 1.0.

The hyperparameter configuration of the method used is the same as that of ILC-SAN, except for the action selection and neuronal models. Specifically, the Gaussian exploration noise with stddev is 0.1 for ILC-SAN, while the initial noise with stddev ( $\sigma_v$  and  $\sigma_s$ ) for our method is  $0.5/\sqrt{N_L}$ , where  $N_L$  denotes the number of neurons in the neural layer, inspired by NoisyNet. The agent uses the noise generation method to generate colored noise instead of Gaussian exploration noise. For NoisySAN, we use pink noise ( $\beta = 1$ ), noisy CLIF neurons with fixed noise parameters and noisy integrated neurons with learnable noise parameters trained by the noise reduction method as default. In addition, the membrane reset voltage of noisy CLIF neurons is 0.0. The details of the training are provided in the appendix.

### 4.2. Comparison with the State-of-the-Art

We compare the performance of our NoisySANs with other SANs, taking the average performance ratio (APR) of different SANs to the corresponding DANs across all the tasks as the measurement standard. This measure can be described as follows:

$$APR(AN) = \frac{1}{N_{\mathcal{T}}} \sum_{task \in \mathcal{T}} \frac{Pref(AN, task)}{Pref(DAN, task)}, \quad (13)$$

where  $\mathcal{T}$  represents a set of tasks, and  $N_{\mathcal{T}} = |\mathcal{T}|$ .  $Pref(AN, task)$  is the max average rewards of the actor

Table 3. Max average rewards over 10 random seeds for NoisySANs with different noisy spiking neurons and  $\beta$  values.

TASK	NOISYSAN			NOISYSAN (ONLY V)			NOISYSAN (ONLY S)		
	$\beta = 0$	$\beta = 1$	$\beta = 2$	$\beta = 0$	$\beta = 1$	$\beta = 2$	$\beta = 0$	$\beta = 1$	$\beta = 2$
ANT-V3	5278	5524	5002	4597	5496	5108	4890	5488	5311
HALFCHEETAH-V3	9694	10723	9750	9696	9626	9780	9900	9377	10025
HOPPER-V3	3004	3356	2770	2822	3457	3458	3039	3181	2777
WALKER2D-V3	4792	4747	4814	4794	4885	4850	4622	4689	4363
HUMANOID-V3	5710	5578	5599	5653	5585	5645	5758	5710	5467
HUMANOIDSTANDUP-V2	158646	161811	153140	155787	160091	174881	167297	167321	159554
INVERTEDDOUBLEPENDULUM-V2	9320	9322	9322	9321	9321	9322	9321	9324	9323
BIPEDALWALKER-V3	270	295	265	195	294	280	280	266	208
APR	112.23%	<b>116.63%</b>	109.67%	104.74%	115.76%	115.70%	112.94%	113.29%	106.10%

Table 4. Max average rewards over 10 random seeds for NoisySANs with different colored noise sequence.

TASK	NOISYSAN	NOISYSAN (RLS)	NOISYSAN (TS)
ANT-V3	5524	5177	5135
HALFCHEETAH-V3	10723	10130	10022
HOPPER-V3	3356	2532	3225
WALKER2D-V3	4747	4510	4608
HUMANOID-V3	5578	5572	5604
HUMANOIDSTANDUP-V2	161811	160020	169095
INVERTEDDOUBLEPENDULUM-V2	9322	9321	9320
BIPEDALWALKER-V3	295	271	301
APR	<b>116.63%</b>	109.87%	115.27%

network over 10 random seeds on the corresponding task, where  $AN$  can be any actor network, such as DAN, PopSAN, MDC-SAN, ILC-SAN, and NoisySAN.

To avoid the impact of training environment and random seeds, all the experiments are under the same experimental setting. We re-run PopSAN and ILC-SAN using their open-source code. Using the best parameters of dynamic neurons given in the paper, we reproduce the MDC-SAN based on the open-source code of PopSAN and re-run it. The complete learning curves of all SANs are shown in the appendix.

As Table 1 shows, NoisySAN obtains the highest APR (116.63%), 16.63% higher than DAN, and 9.41% higher than state-of-the-art SAN, namely ILC-SAN. This is due to the fact that NoisySAN performs remarkably well on some tasks, such as BipedalWalker-v3, where it shows a performance ratio of 152.06%, but at the same time performs slightly worse than DAN on Hopper-v3 (95.34%) and Walker2d-v3 (94.96%). These experimental results demonstrate that our method achieves effective exploration on extensive continuous control tasks from OpenAI gym.

### 4.3. Comparison with the Modified ILC-SAN

In this section, we compare the performance of NoisySANs with ILC-SANs using pink noise or noisy layers. For ILC-SANs using pink noise (ILC-SAN+PN), we use pink noise instead of the Gaussian exploration noise with same stddev. Note that unlike NoisySAN, the pink noise here is used as

action noise and added to the continuous actions outputted by the ILC-SAN. For ILC-SAN using noisy layers (ILC-SAN+NL), we use noisy layers with independent Gaussian noise instead of the linear layers of ILC-SAN, and adopt the same method to initialize the noisy layer (Fortunato et al., 2018). Table 2 shows the results on eight continuous control tasks from OpenAI gym. We can observe that the APR of NoisySAN is 3.75% higher than ILC-SAN+PN and 19.05% higher than ILC-SAN+NL. The complete learning curves are shown in the appendix.

Meanwhile, the introduction of pink noise significantly increase the APR of ILC-SAN (112.88% v.s. 107.22%), which indicates that the ILC-SAN urgently needs improvement in its exploration methods. In addition, the poor performance of ILC-SAN+NL shows that the exploration ability of noisy layers is limited by the firing mechanism of spiking neurons, which also validates our idea that incorporating noise into the spiking neural model is a key issue in developing a general method for exploration of spike-based RL.

### 4.4. Analysis of Noisy Spiking Neurons and Parameter $\beta$

We analyze the impact of different temporally correlated noise processes ( $\beta = 0, 1, 2$ ) and each component of noisy spiking neurons on performance. If noise is only added to the charging dynamics, we call it NoisySAN (only V). If noise is only added to the spike transmission process, we call it NoisySAN (only S). As shown in Table 3, pink noise ( $\beta = 1$ ) achieve better performance than other noise types ( $\beta = 0, 2$ ) on all three NoisySANs with different noisy spiking neurons. For NoisySAN, the APR of pink noise is 4.40% higher than that of white noise ( $\beta = 0$ ) and 6.96% higher than that of red noise ( $\beta = 2$ ), which demonstrates that pink noise can not only be used as default action noise, but is also suitable for our NoisySAN. Moreover, we find that the noise added to the charging dynamics contributes more to the performance gain (115.76% v.s. 113.29%), and the noise added to the spike transmission process can also bring a certain performance gain (116.63% v.s. 115.76%), which further enriches the exploration strategy.

Table 5. Max average rewards over 10 random seeds for NoisySANs with different noise level of non-spiking neurons.

TASK	FFFN	FFFR	FFFL	FFFF
ANT-V3	5206	5524	5400	1946
HALFCHEETAH-V3	9814	10723	9783	8155
HOPPER-V3	3217	3356	2863	2759
WALKER2D-V3	4450	4747	4524	4326
HUMANOID-V3	5723	5578	5583	5544
HUMANOIDSTANDUP-V2	162635	161811	171804	164195
INVERTEDDOUBLEPENDULUM-V2	9320	9322	9322	307
BIPEDALWALKER-V3	297	295	268	275
APR	114.28%	<b>116.63%</b>	112.16%	87.67%

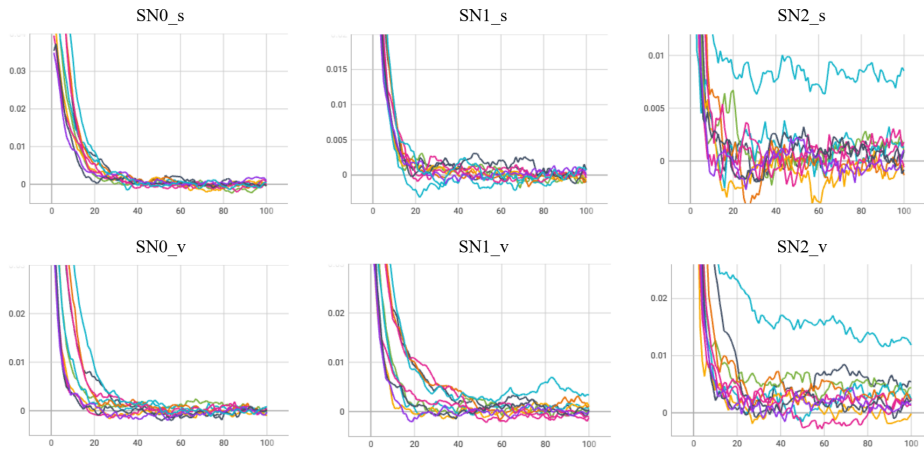


Figure 4. Learning curves of noise parameters in spiking neurons.

Table 6. Max average rewards over 10 random seeds for NoisySANs with different noise parameters for spiking neurons.

TASK	FFFR	LLLR
ANT-V3	5524	5689
HALFCHEETAH-V3	10723	10146
HOPPER-V3	3356	2974
WALKER2D-V3	4747	4228
HUMANOID-V3	5578	5525
HUMANOIDSTANDUP-V2	161811	162805
INVERTEDDOUBLEPENDULUM-V2	9322	9324
BIPEDALWALKER-V3	295	236
APR	<b>116.63%</b>	109.79%

#### 4.5. Analysis of Noise Generation Method

We first evaluate the impact of using colored noise to concatenating action sequence within an episode with spike train within SNNs through ablation study. If we sample colored noise with a length of  $N$  for the action sequence within a episode and use the same noise within the spike-train of

SNNs, we call it NoisySAN (RLS). If we sample colored noise with a length of  $T$  for spike-train within SNNs at each action selection, we call it NoisySAN (TS). In this experiment, we use the default pink noise. As shown in Table 4, NoisySAN achieves better performance than NoisySAN (RLS) and NoisySAN (TS), which demonstrates the effectiveness of our noise generation method. Moreover, we find that introducing time-correlated noise into the spike-train within SNNs contributes more to the performance gain, which can also be demonstrated in the comparison between NoisySAN (TS) and NoisySAN using white noise (115.27% v.s. 112.23%).

#### 4.6. Analysis of Noise Reduction Method

The backbone SNN of NoisySAN contains three noisy spiking neural layers, abbreviated as SN0, SN1, and SN2 in forward propagation order, respectively. The population decoder of NoisySAN contain a noisy non-spiking neural layer, abbreviated as NSN. For noisy spiking neural layers, we can classify them into three categories: fixed noise parameters (abbreviated as F), learnable noise parameters

Table 7. Max average rewards over 10 random seeds for NoisySANs with different partitioning method.

TASK	FFFF	FFFR	FFRR	FRRR	RRRR
ANT-V3	1946	5524	5252	5431	5409
HALFCHEETAH-V3	8155	10723	9725	9616	10236
HOPPER-V3	2759	3356	3420	3229	3468
WALKER2D-V3	4326	4747	4521	4958	4739
HUMANOID-V3	5544	5578	5599	5839	5646
HUMANOIDSTANDUP-V2	164195	161811	168523	169568	167774
INVERTEDDOUBLEPENDULUM-V2	307	9322	9323	9323	9324
BIPEDALWALKER-V3	275	295	237	209	219
APR	87.67%	<b>116.63%</b>	111.47%	111.27%	112.08%

(abbreviated as L), and learnable noise parameters with the noise reduction method (abbreviated as R). For non-spiking neural layer, noise can also be omitted (abbreviated as N). According to the forward propagation order of the network structure, we can represent the default settings of NoisySAN as FFFR. In this section, we use this naming convention to represent different NoisySANs.

We begin by evaluating the effect of different non-spiking neurons. Table 5 shows the performance of FFFN, FFFR, FFFL, and FFFF in ascending order of noise levels. We can find that FFFR obtains the highest APR (116.63%), 2.35% higher than FFFN, 4.47% higher than FFFL, and 28.96% higher than FFFF, which demonstrates the effectiveness of introducing noise and the noise reduction method in non-spiking neurons.

For noisy spiking neurons, we use fixed noise parameters, while for NoisyNet and NROWAN-DQN, the noise parameters are learnable. Therefore, we compared them through experiments. As shown in Table 6, compared with LLLR, FFFR achieve better performance (116.63% v.s. 109.79%). Figure 4 shows the learning curves of noise parameters in spiking neurons, which come from 10 seeds on Walker2d-v3. We analyze the learning curves of each seed for all tasks and find that most of the noise parameters quickly decreased to a extremely small value. Therefore, we can conclude that the rapid decrease in noise parameters in the backbone SNN leads to a decrease in exploration efficiency.

By analyzing the network structure, it is easy to find that the closer the noise is to the output, the fewer spiking neural layers it passes through, and its impact on actions is greater. For the NSN closest to the output, the noise on it can directly affect the action, so it is necessary to introduce the noise reduction method to constrain it, so that the policy in the later stage of training tends to be stable. The experimental results in Table 5 confirm this point. For the spiking neurons in the backbone SNN, especially SNO, the impact of small noise on actions is not significant under the robust binary firing mechanism of SNNs. Therefore, we use fixed noise parameters to enable continuous and effective exploration.

In summary, we need to choose a suitable partitioning method to divide the network into two segments. The first part fixes the noise parameters to ensure effective exploration, while the second part uses the noise reduction method to ensure the final stable policy. As shown in Table 7, the APR of FFFR is 28.96% higher than FFFF, 5.16% higher than FFRR, 5.36% higher than FRRR, and 4.55% higher than RRRR. Therefore, we use fixed noise parameters for spiking neurons in the backbone SNN, and learnable noise parameters trained by the noise reduction method for non-spiking neurons in the population decoder as default. Fortunato *et al.* (2018) pointed out that in certain environments, a larger  $\sigma$  in NoisyNet’s hidden layers has a positive effect. Similarly, we point out that fixing the variance of noisy spiking neurons in the backbone SNN can achieve better performance.

## 5. Conclusion

In this paper, we present NoisySAN, a noisy spiking actor network for exploration that shows significant performance improvements across extensive continuous control tasks from OpenAI gym. By introducing noise into the charging dynamics and spike transmission of spiking neurons, we propose a new spiking neural model. With the help of the noisy spiking neural model, we can introduce the exploration mechanism into the network parameters, bringing more variability to the decisions made by the policy. Inspired by temporal correlation in colored noise, we propose a novel noise generation method to concatenate action sequence within a episode with spike-train within deep SNNs, which further improves the exploration efficiency in various environments. To ensure that the agent ultimately obtains a stable policy, we propose a novel noise reduction method to reduce the noise variance of non-spiking neurons based on tasks and evaluation rewards. We have demonstrated the effectiveness of each of our improvements through detailed experiments, greatly enhancing exploration efficiency and task performance.

## Impact Statements

This paper presents work whose goal is to advance the field of Reinforcement Learning. There are many potential societal consequences of our work, none which we feel must be specifically highlighted here.

## References

- Chen, D., Peng, P., Huang, T., and Tian, Y. Fully spiking actor network with intra-layer connections for reinforcement learning. *arXiv preprint arXiv:2401.05444*, 2024.
- Cox, D. D. and Dean, T. Neural networks and neuroscience-inspired computer vision. *Current Biology*, 24(18):921–929, 2014.
- Eberhard, O., Hollenstein, J., Pinneri, C., and Martius, G. Pink noise is all you need: Colored noise exploration in deep reinforcement learning. In *The Eleventh International Conference on Learning Representations*, 2022.
- Fortunato, M., Azar, M. G., Piot, B., Menick, J., Hessel, M., Osband, I., Graves, A., Mnih, V., Munos, R., Hassabis, D., Pietquin, O., Blundell, C., and Legg, S. Noisy networks for exploration. In *6th International Conference on Learning Representations, ICLR 2018, Vancouver, BC, Canada, April 30 - May 3, 2018, Conference Track Proceedings*. OpenReview.net, 2018. URL <https://openreview.net/forum?id=rywHCPkAW>.
- Fujimoto, S., Hoof, H., and Meger, D. Addressing function approximation error in actor-critic methods. In *International conference on machine learning*, pp. 1587–1596. PMLR, 2018.
- Gu, S., Lillicrap, T., Sutskever, I., and Levine, S. Continuous deep q-learning with model-based acceleration. In *International conference on machine learning*, pp. 2829–2838. PMLR, 2016.
- Haarnoja, T., Zhou, A., Hartikainen, K., Tucker, G., Ha, S., Tan, J., Kumar, V., Zhu, H., Gupta, A., Abbeel, P., et al. Soft actor-critic algorithms and applications. *arXiv preprint arXiv:1812.05905*, 2018.
- Han, S., Zhou, W., Lu, J., Liu, J., and Lü, S. Nrowan-dqn: A stable noisy network with noise reduction and online weight adjustment for exploration. *Expert Systems with Applications*, 203:117343, 2022.
- Hessel, M., Modayil, J., Van Hasselt, H., Schaul, T., Ostrovski, G., Dabney, W., Horgan, D., Piot, B., Azar, M., and Silver, D. Rainbow: Combining improvements in deep reinforcement learning. In *Proceedings of the AAAI conference on artificial intelligence*, volume 32, 2018.
- Hollenstein, J., Auddy, S., Saveriano, M., Renaudo, E., and Piater, J. Action noise in off-policy deep reinforcement learning: Impact on exploration and performance. *arXiv preprint arXiv:2206.03787*, 2022.
- Jiang, C. and Zhang, Y. A noise-based novel strategy for faster snn training. *Neural Computation*, 35(9):1593–1608, 2023.
- Ma, G., Yan, R., and Tang, H. Exploiting noise as a resource for computation and learning in spiking neural networks. *Patterns*, 4(10):100831, 2023. doi: 10.1016/J.PATTER.2023.100831. URL <https://doi.org/10.1016/j.patter.2023.100831>.
- Patel, D., Hazan, H., Saunders, D. J., Siegelmann, H. T., and Kozma, R. Improved robustness of reinforcement learning policies upon conversion to spiking neuronal network platforms applied to atari breakout game. *Neural Networks*, 120:108–115, 2019.
- Plappert, M., Houthoofd, R., Dhariwal, P., Sidor, S., Chen, R. Y., Chen, X., Asfour, T., Abbeel, P., and Andrychowicz, M. Parameter space noise for exploration. In *6th International Conference on Learning Representations, ICLR 2018, Vancouver, BC, Canada, April 30 - May 3, 2018, Conference Track Proceedings*. OpenReview.net, 2018. URL <https://openreview.net/forum?id=ByBA12eAZ>.
- Roy, K., Jaiswal, A., and Panda, P. Towards spike-based machine intelligence with neuromorphic computing. *Nature*, 575(7784):607–617, 2019.
- Schrittwieser, J., Antonoglou, I., Hubert, T., Simonyan, K., Sifre, L., Schmitt, S., Guez, A., Lockhart, E., Hassabis, D., Graepel, T., et al. Mastering atari, go, chess and shogi by planning with a learned model. *Nature*, 588(7839):604–609, 2020.
- Stein, R. B., Gossen, E. R., and Jones, K. E. Neuronal variability: noise or part of the signal? *Nature Reviews Neuroscience*, 6(5):389–397, 2005.
- Sutton, R. S. and Barto, A. G. *Reinforcement learning: An introduction*. MIT press, 2018.
- Tang, G., Kumar, N., and Michmizos, K. P. Reinforcement co-learning of deep and spiking neural networks for energy-efficient mapless navigation with neuromorphic hardware. In *2020 IEEE/RSJ International Conference on Intelligent Robots and Systems (IROS)*, pp. 6090–6097. IEEE, 2020.
- Tang, G., Kumar, N., Yoo, R., and Michmizos, K. Deep reinforcement learning with population-coded spiking neural network for continuous control. In *Conference on Robot Learning*, pp. 2016–2029. PMLR, 2021.

Verveen, A. and DeFelice, L. Membrane noise. *Progress in biophysics and molecular biology*, 28:189–265, 1974.

Zhang, D., Zhang, T., Jia, S., and Xu, B. Multiscale dynamic coding improved spiking actor network for reinforcement learning. In *Thirty-sixth AAAI conference on artificial intelligence*, 2022.

Zhang, Z., Jiang, J., Chen, M., Wang, Z., Peng, Y., and Yu, Z. A novel noise injection-based training scheme for better model robustness. *arXiv preprint arXiv:2302.10802*, 2023.

## A. Training Hyper-parameters

For tasks with  $N$ -dimensional state and  $M$ -dimensional action, hyper-parameter configurations for the methods used subsequently are as follows: the deep critic network is  $(N + M, 256, \text{relu}, 256, \text{relu}, 1)$ ; the NoisySAN is  $(N \cdot P_{in}, 256, \text{noisy CLIF neurons}, 256, \text{noisy CLIF neurons}, M \cdot P_{out}, \text{noisy CLIF neurons}, M, \text{noisy integrated neurons})$ , the population size for each state  $P_{in}$  and action dimension  $P_{out}$  is 10; the learning rate of the deep critic network is  $1e-3$ ; the learning rate of the NoisySAN is  $1e-4$ ; the reward discount factor is 0.99; the initial noise with stddev ( $\sigma_v$  and  $\sigma_s$ ) for our method is  $0.5/\sqrt{N_L}$ , where  $N_L$  denotes the number of neurons in the neural layer; the Gaussian smoothing noise for target policy with stddev is 0.2; the maximum length of replay buffer is  $1e6$ ; the soft target update factor is 0.005; the batch size is 100; the noise clip is 0.5; the policy delay factor is 2; the factor  $k_0$  is 1.0.

For noisy CLIF neurons, we use the same hyper-parameters as the open-source code of PopSAN, so the membrane reset voltage  $V_{reset}$  is 0.0, the threshold voltage  $V_{th}$  is 0.5, the current decay factor  $\alpha_C$  is 0.5, the voltage decay factor  $\alpha_V$  is 0.75, and the threshold window  $w$  is 0.5.

## B. Comparison with the State-of-the-Art

The complete learning curves of NoisySAN, PopSAN, MDC-SAN, and ILC-SAN across all tasks are shown in Figure 5. As we can see, NoisySAN achieves better performance on Ant-v3, Hopper-v3, Walker2d-v3 and BipedalWalker-v3. Especially on BipedalWalker-v3, NoisySAN performs remarkably well. In addition, NoisySAN achieves comparable performance on other tasks.

## C. Comparison with the Modified ILC-SAN

The complete learning curves of NoisySAN and ILC-SAN using pink noise or noisy layers across all tasks are shown in Figure 6. As we can see, NoisySAN achieves better performance on HalfCheetah-v3 and BipedalWalker-v3. Especially on BipedalWalker-v3, NoisySAN performs remarkably well. On HumanoidStandup-v2, the performance of NoisySAN is slightly inferior to ILC-SAN using pink noise. Moreover, the performance of NoisySAN on other tasks is at the same level as ILC-SAN using pink noise, and the performance of ILC-SAN using noisy layers is far inferior to the other two.

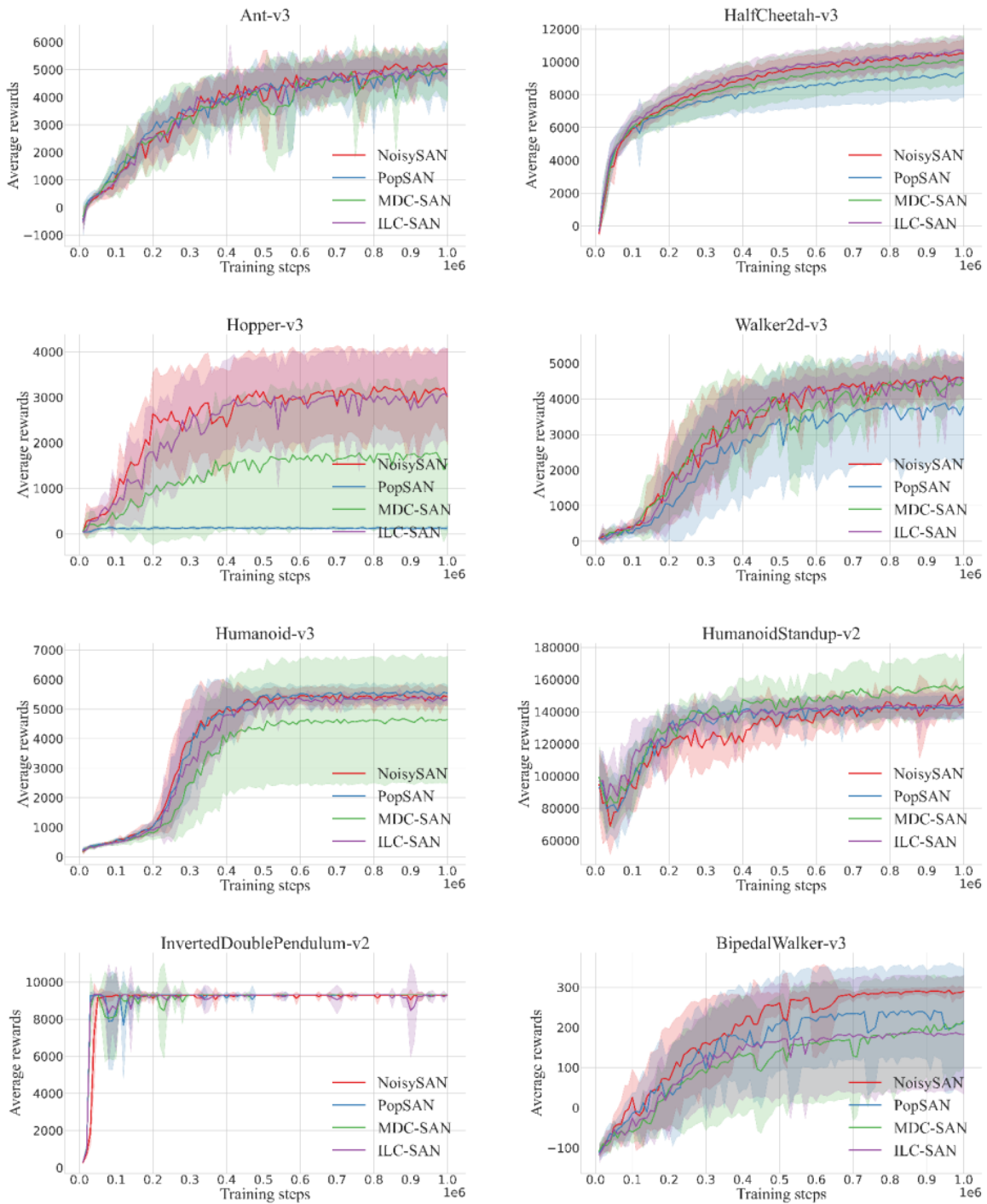


Figure 5. The comparison of average rewards for NoisySAN, PopSAN, MDC-SAN, and ILC-SAN over 10 random seeds. The shaded area represents half the value of the standard deviation, and the curves are smoothed for clarity.

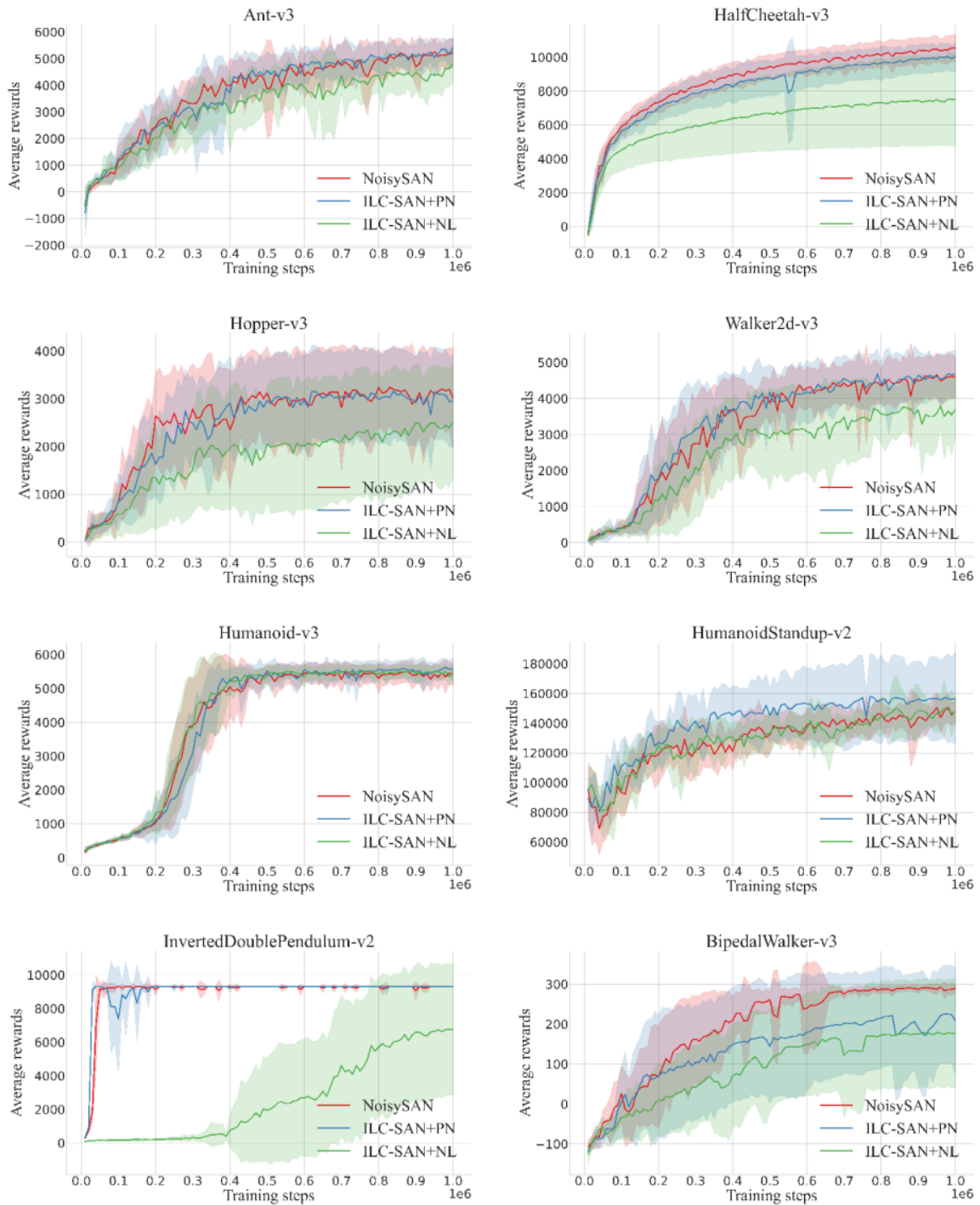


Figure 6. The comparison of average rewards for NoisySAN and ILC-SAN using pink noise or noisy layers over 10 random seeds. The shaded area represents half the value of the standard deviation, and the curves are smoothed for clarity.